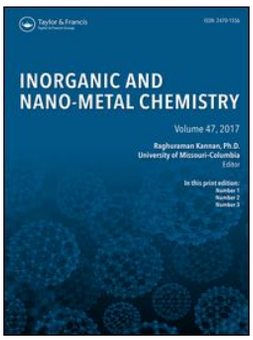

Inorganic and Nano-Metal Chemistry

ISSN: 2470-1556 (Print) 2470-1564 (Online) Journal homepage: http://www.tandfonline.com/loi/lsrt21

Synthesis, characterization, and biological activity of new mixed ligand transition metal complexes of glutamine, glutaric, and glutamic acid with nitrogen based ligands

Laila H. Abdel-Rahman, Ahmed M. Abu-Dief, Nabawia M. Ismail & Mohamed Ismael

To cite this article: Laila H. Abdel-Rahman, Ahmed M. Abu-Dief, Nabawia M. Ismail & Mohamed Ismael (2017) Synthesis, characterization, and biological activity of new mixed ligand transition metal complexes of glutamine, glutaric, and glutamic acid with nitrogen based ligands, Inorganic and Nano-Metal Chemistry, 47:3, 467-480, DOI: 10.1080/15533174.2015.1137057

To link to this article: http://dx.doi.org/10.1080/15533174.2015.1137057

Published online: 04 Nov 2017.

INORGANIC AND NANO-METAL CHEMISTRY
2017, VOL. 47, NO. 3, 467–480
http://dx.doi.org/10.1080/15533174.2015.1137057

Taylor & Francis
Taylor & Francis Group

Synthesis, characterization, and biological activity of new mixed ligand transition metal complexes of glutamine, glutaric, and glutamic acid with nitrogen based ligands

Laila H. Abdel-Rahman[a], Ahmed M. Abu-Dief[a,b], Nabawia M. Ismail[a], and Mohamed Ismael[a]

[a]Chemistry Department, Faculty of Science, Sohag University, Sohag, Egypt; [b]Departamento de Quimica Organica e Inorganica, Faculad de Quimica, Universdad de Oviedo, Oviedo, Spain

ABSTRACT

A new series of Cu(II), Co(II), Ni(II), and Fe(II) ternary complexes of glutamine, glutaric, and glutamic acid with imidazole derivatives have been synthesized. The nature of the bonding and the stereochemistry of the complexes have been deduced from elemental analyses, infrared and electronic spectra, conductivity measurements, and thermogravimetric analysis. The structure of $[Co(glu)(IMI)_2]$ and $[Fe(glu)(IMI)_2(H_2O)_2]$ complexes was validated using quantum mechanics calculations based on accurate DFT methods. Calculations revealed that both complexes had distorted tetrahedral geometry. In case of $[Co(glu)(IMI)_2]$, glu ligand was coordinated through the terminal part which consists of carboxylate and amine groups. The formation constants of mixed ligand complexes of copper (II) and nickel (II) with glutamic-glutamine-glutaric as primary ligands and imidazole or its derivatives as secondary ligands have been determined by pH metric technique in aqueous medium. The data obtained were used to evaluate the values of metal-ligand stability constants using Irving-Rossotti titration technique. Mixed ligand complexes studies of these metal ions have been carried pH-metrically at the same conditions. In addition, the interaction of these complexes with calf-thymus DNA (CT-DNA) was investigated at pH = 7.2 by using UV–vis absorption and viscosity measurements. Results indicated that the investigated complexes strongly bind to CT-DNA via intercalative mode. Moreover, the prepared compounds are screened for their *in vitro* antibacterial activity against two types of bacteria, *Pseudomonas aeruginosa* and *Bacillus cereus*. In general, based on the data obtained in this study, the synthesized metal complexes might be taken into consideration as promising antibacterial compounds.

ARTICLE HISTORY
Received 14 May 2015
Accepted 27 December 2015

KEYWORDS
Ternary complexes; imidazol; glutamine; glutamic acid; glutaric acid; CT-DNA

Introduction

Coordination compounds exhibit different characteristic properties that depend on the metal ion to which they are bound. The nature of the metal as well as the type of ligand, etc. these metal complexes have found extensive application in various fields of human interest. The amino acids have significant importance among the chemicals since they are the "building blocks" of the living systems. Besides, they find application in many fields (and in industry) including foods, animal feed supplements, and pharmaceutical production. In biological fluids where metal ions are present in trace quantities, some ligands show a marked tendency to compete for metal ions. Obviously, studies on mixed ligand formation under physiological conditions are important. It is known that metal ions are important for numerous biochemical reactions. For example, enzymes work only in the presence of such metal ions. The metal ion complexes of many amino acids have been investigated.[1–3] The behavior of various materials functionalized with polypeptides and other molecules is a topic of interest because of its applications in affinity separations, biosensors, and other applications including site-specific interactions.[4] An example of the latter involves the removal of heavy metals from aqueous solutions.[5] These sorbents are made of a variety of materials containing different functional groups. The advantage of affinity separations is that they may be tailored for the desired selectivity and capacity. The functionalization of materials is of vital importance for the production of new materials with specific properties. L-glutamate is key molecule in cellular metabolism (cf. Scheme 1). In humans, dietary proteins are broken down by digestion into amino acids, which serve as metabolic fuel for other functional roles in the body. On the basis of this, the essential role of glutamine is interesting to study the interaction between other metal ions with glutamine and related compounds.

Changes in the concentration of free L-amino acids, including aspartic and glutamic acids in the brain tissue of Alzheimer sufferers with respect to healthy persons, permit evaluation of the degree of degradation of nerve tissue caused by this disease.[6,7] It is well known that DNA is a useful target for many anticancer drugs and the effectiveness mainly depends on the mode and affinity of the binding between the drugs and DNA. It is reported that the transition metal complexes can interact non-covalently with nucleic acids and act as active anticancer drugs[8] in the mode of intercalation, groove binding, or

CONTACT Ahmed M. Abu-Dief ahmed_benzoic@yahoo.com Chemistry Department, Faculty of Science, Sohag University, 82534, Sohag, Egypt.
Color versions of one or more of the figures in the article can be found online at www.tandfonline.com/lsrt.
Supplemental data for this article is available at the publisher's website.

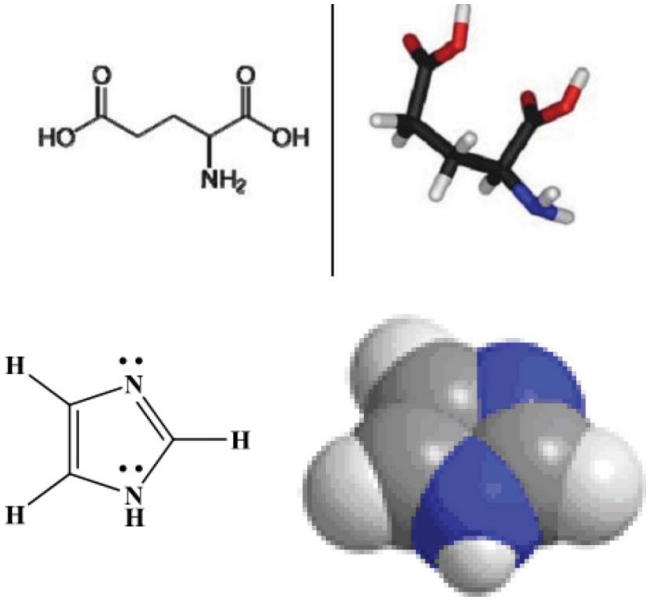

Scheme 1. Structure of glutamine and imidazole.

external electrostatic binding,[9,10] so the research concerning the interaction of transition metal complexes and DNA interested many researchers over the past decades.[11–13] Thus, the present work stems from our interests to develop this chemistry further by synthesizing new ternary Cu(II), Co(II), Ni(II), and Fe(II) complexes of a-amino acid L-glutamine, glutamic, and glutaric acid with N,N-donor heterocyclic bases. This amino acid with its terminal –C(= O)–NH_2 group has the potential to form significant hydrogen bonding interactions with the double-stranded (ds) DNA and could show good DNA-binding propensity. Mixed–ligands complexes containing ligand imidazole (IMI; cf. Scheme 1) are of considerable interest because they provide a binding site for the interaction of several proteins and DNA with metal ion.

Experimental

Materials

L-glutamine, L-glutamic acid, L-glutaric acid, potassium hydrogen phthalate, sodium hydroxide, and EDTA (extra pure) were purchased from Merck. Metal salts Cu(II), Co(II), and Ni(II), and Fe(II) nitrates were obtained from Sigma-Aldrich, Germany.

Synthesis of metal chelates

An ethanolic solution (10 mL) of imidazole (0.27 g, 4 mmol) was added to a solution of copper(II), cobalt(II), nickel(II), and iron(II) nitrate (0.19 g, 1 mmol) in water (30 mL) containing (0.66g, 2 mmol) or glutamic acid, glutamine (0.29 g, 2 mmol), and glutaric acid (0.26 g, 2 mmol). Aqueous concentrated NaOH was added to maintain the pH at 8. Upon slow evaporation, the solid complexes were separated. The proposed structures of the prepared complexes are shown in Scheme 2. The results of molar conductance, maximum absorbance, decomposition temperature, yields, and the elemental analyses of all complexes are listed in Table 1.

Instrumentation

The complexes composition was derived from C, H, and N content as determined with Perkin Elmer 40c elemental analyzer (Microanalytical Centre at Cairo University, Egypt). Melting points were measured on an Electrothermal 9200 melting point apparatus. The molar conductance of 10^{-3} M solutions was measured with JENWAY 4320 conductometer at 298 K. IR spectra were recorded with Shimadzu FTIR 8101 at 4000–400 cm^{-1} (KBr). Electronic absorption spectra of the complexes in methanol were recorded with Jasco V-530 spectrophotometer (200–800 nm, 10 mm quartz cell). The spectrometer thermostated cell holder was supplied by an ultra thermostat water circulator (CRIOTERM 190) to control the temperature at 25°C. Thermogravimetric analysis was carried out on a Mettler-Toledo TGA/SDT A 851 thermal analyzer in the range 30–800°C at a heating rate of 10°C/min under air condition. Quantum mechanics (QM) calculations were used to verify the 3D structure of the complex structures. Moreover, calculations were used to estimate the chemical reactivity of the complexes based on the electronic structure analysis. Density functional theory (DFT) calculations were performed for optimization using B3LYP functional with 6-311G (d, p) bases set implemented on Gaussian package.[14,15] Calculations were done for glutamine (glu), IMI, and [M(glu)$(IMI)_2$] models where M is Co^{2+} and Fe^{2+} ions.

pH titrations

Potassium hydrogen phthalate and standard solutions of sodium hydroxide (Titrasol), nitric acid, EDTA, and the buffer solutions of pH 4.0, 7.0, and 9.0 were all from Merck. All solutions were prepared with deionized water. Water was purified by Milil-Q water purification system.

1. (0.002 M) HNO_3.
2. (0.002 M) HNO_3 + (0.004 M) amino acid.
3. (0.002 M) HNO_3 + (0.004 M) amino acid + (.002 M) metal.
4. (0.002 M) HNO_3 + (0.004 M) amino acid + (0.002 M) metal + (0.004 M) secondary ligand.
5. (0.002 M) HNO_3+ (0.004 M) secondary ligand.
6. (0.002 M) HNO_3 + (0.004M) secondary ligand+ (0.002 M) metal.

The ratio of metal (M) to primary ligand (A) to secondary ligand (L) was maintained at 1:1:1 in each of the ternary systems.

The formation constant values of the binary and ternary complexes were calculated using a computer program based on the formula of Irving and Rossetti equation.

Reagents and apparatus

Carbonate-free sodium hydroxide 0.03 M was prepared and standardized against sodium hydrogen phthalate and a standard solution of nitric acid 0.5 mM. M(II) nitrate solution (0.03 M) was prepared by dissolving the above substance in water and standardized with standard solution of EDTA 0.1 M. All pH titrations were performed using a Metrohm 794 basic automatic titrator (Titrino), coupled with a thermostating bath Hero at 25°C (±0.1°C) and a Metrohm combined glass electrode (Ag/AgCl). The pH meter was calibrated with Merck standard buffer solutions (4.0, 7.0, and 9.0).

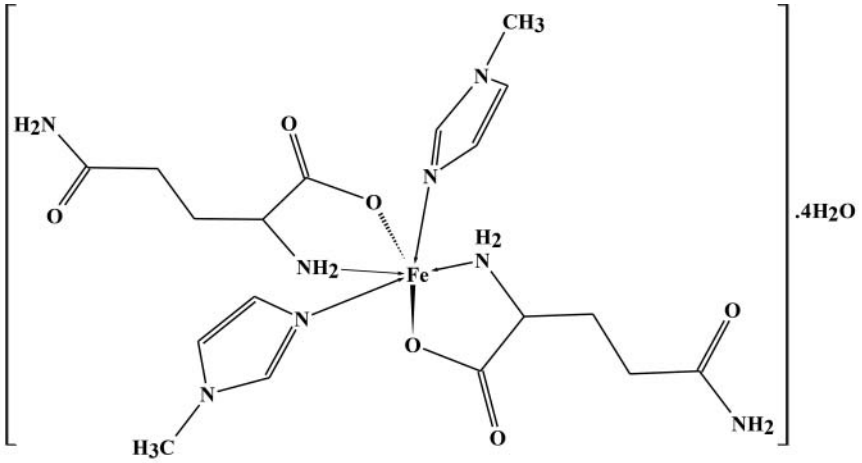

[Fe(Glutn)$_2$(IMI)$_2$].4H$_2$O

GIMFe

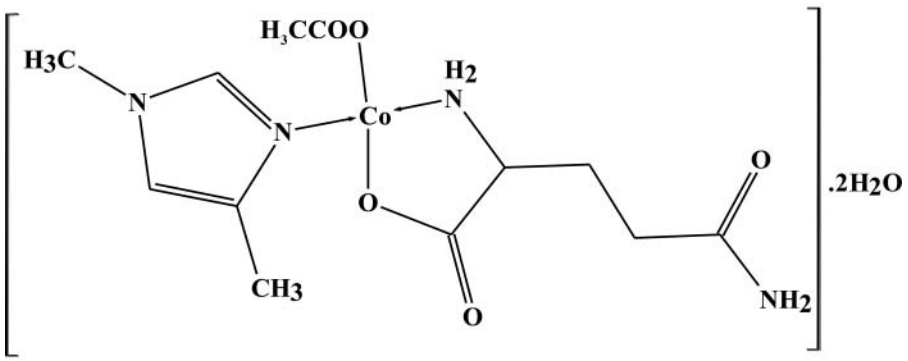

[Co(Glutn)(IMI)(CH$_3$COO)].2H$_2$O

GIMCo

Scheme 2. Proposed structure of the prepared complexes.

DNA binding studies

All the DNA binding experiments, involving the interaction of the complexes with calf-thymus DNA (CT-DNA), were carried out under physiological conditions in Tris–HCl buffer (50 mM Tris–HCl, pH 7.2) containing 5% DMF at room temperature. A solution of CT-DNA in the buffer gave a ratio of UV absorbance at 260 and 280 nm of about 1.89:1, indicating the CT-DNA sufficiently free from protein.[13,16,17] The CT-DNA concentration per nucleotide was determined by absorption spectroscopy using the molar absorption coefficient of 6600 M^{-1} cm^{-1} at 260 nm.

Absorption spectroscopic studies

Absorption titration experiments were performed by maintaining the metal complex concentration as constant at 50μM while gradually increasing the concentration of the CT-DNA within 40–400 μ M. While measuring the absorption spectrum, equal quantity of CT-DNA was added to both the complex solution and the reference solution to eliminate the absorbance of CT-DNA itself. The solutions were mixed for 5 min, and then the absorption spectra were recorded. The titration process was repeated until there was no change in the spectra (binding saturation achieved). The changes in the metal complex concentration due to complexes dilution at the end of each titration were negligible. From the absorption data, the intrinsic binding constant K_b was determined from of plotting [DNA]/(ε_a – ε_f) versus [DNA] the following equation[16,17]:

$$\frac{[DNA]}{(\varepsilon_a - \varepsilon_f)} = \frac{[DNA]}{(\varepsilon_b - \varepsilon_f)} + \frac{1}{[K_b\,(\varepsilon_b - \varepsilon_f)]}$$

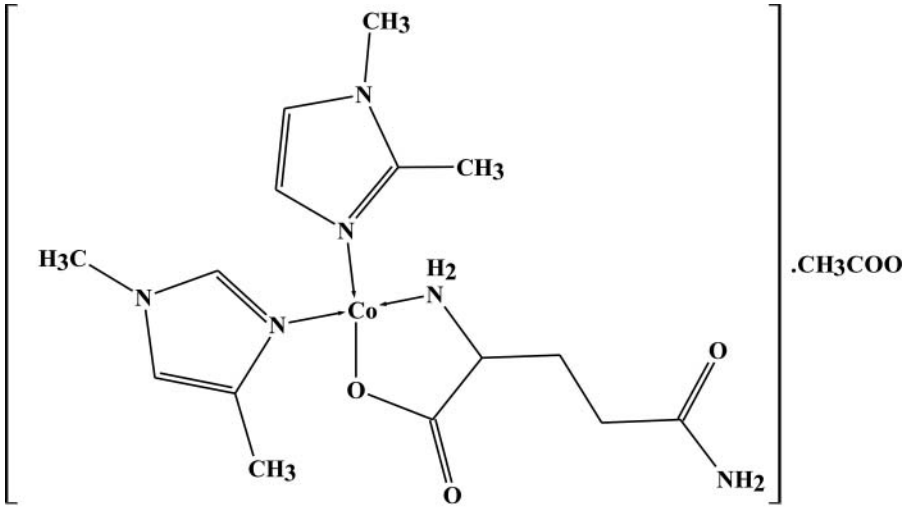

[Co(Glutn)(DMI)$_2$].CH$_3$COO
GDMCo

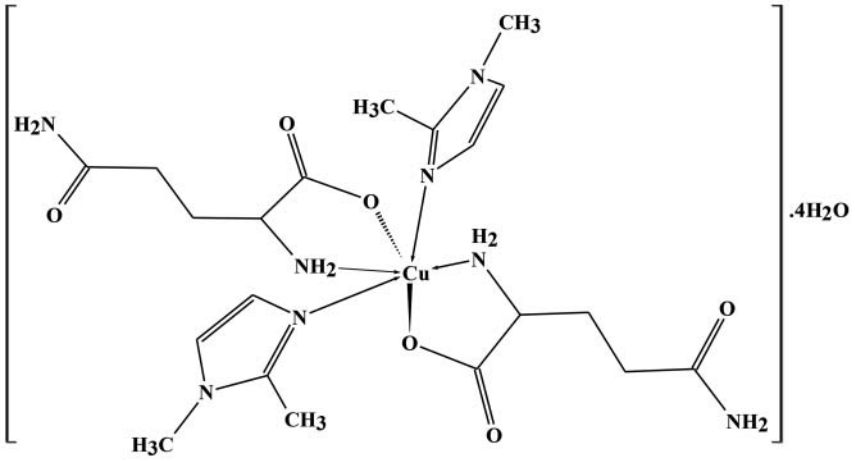

[Cu(Glutn)$_2$(DMI)$_2$].4H$_2$O

Scheme 2. (Continued).

where [DNA] is the concentration of DNA in base pairs, and the apparent absorption coefficients ε_a, ε_f, and ε_b correspond to A_{obsd}/[complex], the extinction coefficient for the free complex, and extinction coefficient for the complex in fully bound form, respectively.

DNA binding using viscosity measurements

Viscosity experiments were carried out using an ALPHA L Fungi lab rotational viscometer equipped with an 18 mL LCP spindle and the measurements were performed at 100 rpm. The viscosity of DNA solution has been measured in the presence of increasing amounts of complex. The relation between the relative solution viscosity ($\eta/\eta 0$) and DNA length (L/L^0) is given by the equation $L/L^0 = (\eta/\eta 0)^{1/3}$, where L^0 denotes the apparent molecular length in the absence of the compound. The obtained data are presented as $(\eta/\eta 0)^{1/3}$ versus r, where η is the viscosity of DNA in the presence of complex and $\eta 0$ is the viscosity of DNA alone in buffer solution.[13,16–18]

Pharmacology: In vitro antibacterial assay of the prepared complexes

All the synthesized Schiff base ligands and their corresponding metal (II) complexes were screened *in vitro* for their antibacterial activity against two types of the pathogenic bacteria, one Gram-negative (*Pseudomonas aeruginosa*) and the other Gram-positive (*Bacillus cereus*) bacterial strains using agar well diffusion method.[17,19] Ofloxacin and ciprofloxacin were used as standards for antibacterial activity. Each compound was

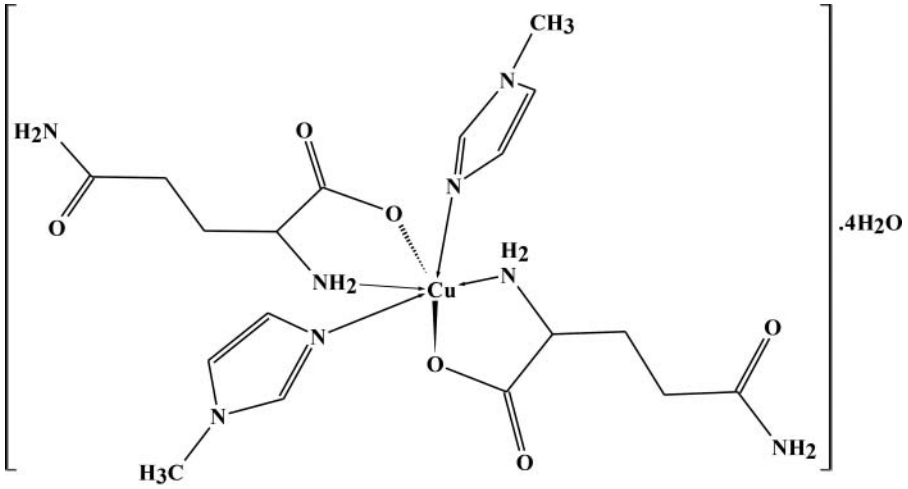

[Cu(Glutn)$_2$(MIMI)$_2$].4H$_2$O

GMICu

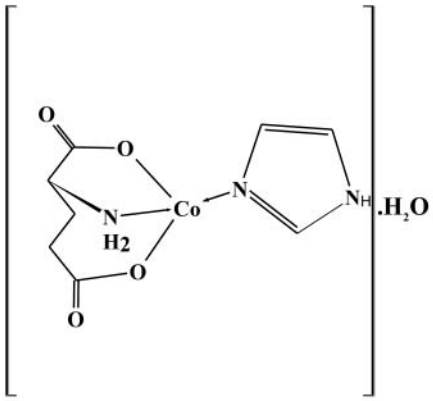

[Co(Glutamic)(IMI)].H$_2$O

GCIMCo

Scheme 2. (Continued).

dissolved in dimethyl sulfoxide at different concentrations (5, 10, and 20 mg/mL). DMSO was used as a solvent and also for control. DMSO was found to have no antimicrobial activity against any of the test organisms. 1 cm^3 of a 24 h broth culture containing 106 CFU/cm^3 was placed in sterile Petri dishes. Molten nutrient agar (15 cm^3) maintained at *ca*. 45°C was then poured into the Petri dishes and allowed to solidify. Then holes of 6 mm diameter were formed in the agar using a sterile cork borer and these holes were completely filled with the test solutions. The plates were incubated for 24 h at 37°C. The zones of inhibition based upon zone size around the wells were measured.

Results and discussion

Characterization of the prepared ternary complexes

All the complexes are stable at room temperature and non-hygroscopic. On heating, they decompose at high temperatures. The complexes are insoluble in water but soluble in DMSO. Examination of the microanalytical data of the differently synthesized with Fe(II), Co(II), Ni(II), and Cu(II) ternary amino acid complexes with IMI, MIMI, and DMI (Table 1) revealed their proposed stoichiometric ratios. The measured molar conductance values of 10^{-3} to 10^{-4} molar solutions of the prepared complexes in ethanol were found to be in the range 8.50–32.70 ohm^{-1} cm^{-2} mol^{-1} (Table 1). The nonelectrolytic nature of the prepared complexes can be accounted by the deprotontation of the carboxylic group of the ligands when it is coordinated to metal ion (cf. Scheme 1).[13]

Thermogravimetric analysis for the prepared complexes

The thermogravimetric analyses (TG) were performed for the ternary complexes under investigation to verify the amount of solvent molecules that may exist in these complexes. Lattice water is lost at lower temperature regions between 60 and 120°C, whereas the loss of coordinated water requires 150°C or

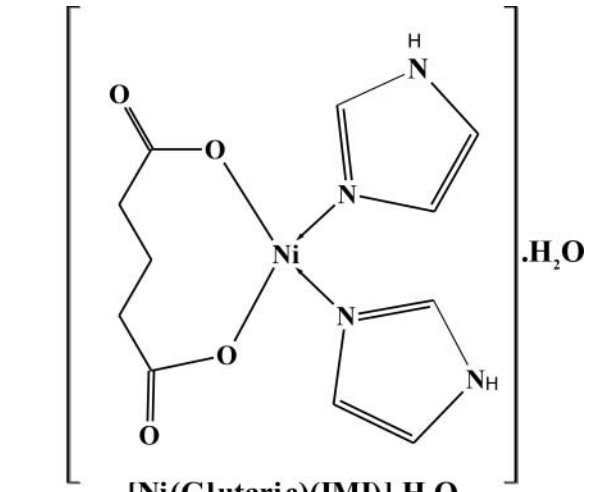

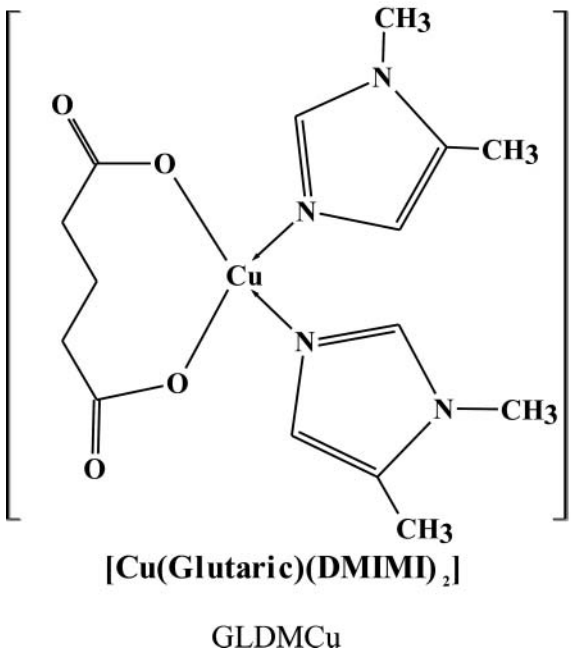

Scheme 2. The proposed structures for the prepared complexes.

above. The TG data GIMFe and GMICu complexes (cf. Table 2) show one decomposition step in the temperature range 25–130°C with 13.10% and 12.80% loss, respectively, which is probably due to the removal of four water molecules that are likely to be of hydration, in agreement with the elemental analysis (Table 1). GCIMCo and GLIMNi complexes display an initial slow weight loss of 5.92% and 7.15% in the range 20–140°C, respectively, which is in accordance with the loss of one crystallized water molecule.

IR spectra

Unfortunately we could not take advantage of the powerful structure elucidation technique, X-ray diffraction; however, we recorded the infrared spectra in order to elucidate the nature of the ligands to metal ion bonding. The IR spectra of the complexes showed characteristic bands due to functional groups of ligands. The more relevant IR bands are reported in Table 3. The infrared spectra of Fe(II), Co(II), Ni(II), and Cu(II) are characterized by a broad band in the 3442–3360 cm^{-1} region, which can be ascribed to the stretching vibrations of water molecules present in the lattice consistent with elemental and thermogravimetric analyses.[13,17] The IR band spectra of all complexes are in the range 3150–3107 cm^{-1} corresponding to the stretching vibration of the uncoordinated NH group of glutamine, glutamic or imidazole moiety.[20] Furthermore, The distinct band appearing in the region of 1630–1593 cm^{-1} in the IR spectra of all complexes (Table 3), is a typical for asymmetric vibration of the coordinated carboxylate group, confirmed the coordination of the glutamine, glutamic, and glutaric acids through the carboxylic oxygen.[21] Accordingly, the absence of any band in the region 1750–1700 cm^{-1} in the IR spectra of the isolated ternary complexes suggest the coordination of the COO– group of the glutamine, glutamic, and glutaric acids to the central metal ions. For all complexes the band appeared in the region 1437–1391 cm^{-1} can likely be ascribed to the symmetric vibration of the coordinated carboxylate group. New bands appeared in all complexes in the frequency ranges 657–599 cm^{-1} and 502–435 cm^{-1}, which are attributed to $\upsilon_{M\text{-}N}$ and $\upsilon_{M\text{-}O}$, respectively.[13,16,17]

Molecular electronic spectra

The major features of electronic absorption spectra, molar extinction coefficients, and the band assignment of the different bands of prepared complexes with Fe(II), Co(II), Ni(II), and Cu (II) (recorded in DMSO media, $c = 1\times 10^{-3}$ mol/L, at 298 K) are listed in Table 3. The spectra of the complexes are dominated by intense intraligand bands centered at λ_{max} = 340–375 nm (ε_{max} = 1240–787.5 mol^{-1} cm^2) and charge transfer bands centered at 345–410 nm (ε_{max} = 975–762 mol^{-1} cm^2), since it is known that metals are capable of forming dπ–pπ bonds with ligands containing nitrogen and oxygen as donor atoms.[22] Furthermore, the L → MCT band is followed by a long and a broad band lies in the region 400–430 nm (ε_{max} = 800–983 mol^{-1} cm^2). This band could be mainly attributed to the d → d transition in the octahedral structure of the prepared complexes.[13,16,17,22]

Molecular calculations

In the absence of an X-ray crystal structure data the three-dimensional structure of the molecules cannot be entirely unambiguous. However, recent major advances in the computational chemistry tools provide an alternative, albeit approximate, approach for obtaining the three dimensional structures of the compounds. Optimizing Glu showed that the structure consists of intramolecular H-bond between the carboxylic group (donor) and anime group (acceptor) with H-bond length of 2.16 Å. This orientation enables the di-dentate coordination with metal ions. Imidazole optimization gave planner structure with C_s point group symmetry. Optimized structures of both models are shown in Figures S1 and S2. Figure 1 shows the optimized structures of [Co(glu)$(IMI)_2$] and [Fe(glu)$(IMI)_2(H_2O)_2$] complexes, and the calculated M-L geometry parameters are listed in Table 4. Calculations revealed that both complexes have distorted tetrahedral geometry. In case of [Co(glu)

Table 1. Elemental analyses, decomposition temperature, and molar conductance results of the different mixed ligand complexes of Co(II), Ni(II), Cu(II), and Fe(II) amino and carboxylic acids with imidazole derivatives.

Amino or carboxylic acids	Compound	Abbreviation molecular formula	M.Wt	Decomp.temp.	Conductance	Found (Calcd.)		
						C	H	N
Glutamine 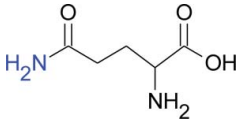	$[Fe(Glutn)_2(IMI)_2].4H_2O$	GIMFe $C_{16}H_{34}N_8O_{10}Fe$	**554.21**	**>300**	**19.55**	**34.22 (34.47)**	**6.37 (6.14)**	**20.34 (20.21)**
	$[Co(Glutn)(IMI)(CH_3COO)].2H_2O$	GIMCo $C_{10}H_{20}N_4O_7Co$	**367.15**	**180**	**13.50**	**32.95 (32.68)**	**5.67 (5.44)**	**15.41 15.25)**
	$[Co(Glutn)(DMI)_2].CH_3COO$	GDMCo $C_{16}H_{28}N_6O_5Co$	**456.33**	**218**	**32.70**	**42.40 (42.07)**	**6.36 (6.14)**	**18.71 (18.41**
	$[Cu(Glutn)_2(DMI)_2].4H_2O$	GDMCu $C_{20}H_{42}N_8O_{10}Cu$	**617.54**	**260**	**8.50**	**38.95 (38.86)**	**7.10 (6.80)**	**18.16 (18.13)**
	$[Cu(Glutn)_2(MIMI)_2].4H_2O$	GMICu $C_{18}H_{42}N_8O_{10}Cu$	**593.33**	**200**	**13.40**	**36.49 (36.40)**	**6.91 (7.08)**	**27.32 (26.97)**
Glutamic acid 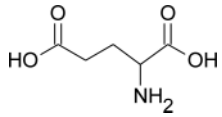	$[Co(Glutc)(IMI)].H_2O$	GCIMCo $C_8H_{13}N_3O_5Co$	**290.14**	**235**	**11.50**	**32.86 (33.09)**	**4.93 (4.48)**	**14.37 (14.48)**
Glutaric acid 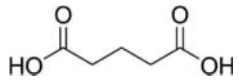	$[Ni(Glutar)(IMI)].H_2O$	GLIMNi $C_{11}H_{16}N_4O_5Ni$	**342.78**	**230**	**14.30**	**38.24 (38.51)**	**5.07 (4.68)**	**15.92 (16.33)**
	$[Cu(Glutar)(DMIMI)_2]$	GLDMCu $C_{15}H_{22}N_4O_4Cu$	**385.54**	**>300**	**16.00**	**46.45 (46.69)**	**5.94 (5.71)**	**14.84 (14.52)**

Glutn = **gultamine;** Glutar = **glutaric acid;** Glutc = **glutamic acid; IMI = imidazole; MIMI = methyl imidazole; DMIMI = dimethyl imidazole.**

Table 2. TGA data of the studied complexes.

Complex	Temperature	Fragment loss		Weight loss	
		Molecular formula	Molecular weight	Theoretical	Found
$[Fe(Glutn)_2(IMI)_2].4H_2O$ GIMFe	25–130°C	$4H_2O$	72	12.94	13.1
	130–225°C	$C_4N_2OH_9$	101	18.15	17.65
	225–450°C	$C_3N_2H_4$	68	12.23	11.94
	450–675°C	$C_8N_4O_3H_{13}$	213	38.49	39.21
Remaining		Fe(II) + CO_2	100	17.97	18.02
$[Co(Glutn)(IMI)CH_3COO].2H_2O$ GIMCo	28–120 °C	$2H_2O$	36	9.81	10.04
	120–286°C	CH_3COO	59	13.89	12.89
	286–415°C	$C_5H_9N_2O_2$	129	35.14	35.5
	415–690°C	$C_3H_4N_2$	68	18.54	19
Remaining		CoO	75	16.04	16.5
$[[Co(Glutn)(DMIMI)_2].CH_3COO$ GDMCo	26–160 °C	CH_3COO	59	12.94	13.02
	160–405°C	$C_5H_9N_2O_2$	129	28.27	27.5
	405–695°C	$C_5N_2H_8$	96	12.23	11.97
Remaining		CoO	75	16.41	17.11
$[Cu(Glutar)(DMIMI)_2]$ GLDMCu	25-315°C	$C_9N_2O_2H_{14}$	182	45.32	44.9
	316–685°C	$C_5N_2H_8$	96	23.94	22.98
Remaining		Cu(II) +CO_2	108	23.74	23.13
$[Co(Glutamic)(IMI)].H_2O$ GCIMCo	28–120 °C	H_2O	18	6.23	5.92
	120–450°C	$C_4O_2NH_7$	101	34.96	33.98
	450–680°C	$C_3N_2H_3$	67	23.19	23.43
Remaining		Co+CO_2	103	35.62	36.11
$[Cu(Glutn)_2(DMI)_2].4H_2O$ GMICu	28.5–285.3°C	$4H_2O$ +$C_{10}H_{16}O_3N_4$	312	50.67	50.16
	286–418°C	$C_4H_8N_2O$	100	17.07	18.9
	419–628°C	$C_5N_2H_8$	96	13.88	12.39
Remaining		Cu+CO_2	108	18.17	18.54
$[Ni(Glutar)(IMI)].H_2O$ GLIMNi	26–142°C	H_2O	18	5.25	7.16
	143–362°C	$C_3N_2H_3O$	83	24.213	25.6
	363–387°C	CO	28	8.17	8.96
	388–457°C	CH_3	15	4.38	3.9
	458–694°C	$C_5H6N_2O_2$	126	36.4	34.9
Remaining		Ni	59	17.12	19.48
$[Cu(Glutn)_2(MIMI)_2].4H_2O$ GMICu	25–114°C	$4H_2O$	72	12.13	12.5
	116–290°C	$C_9H_{14}O_3N_4$	226	38.09	39
	290–420°C	$C_4H_8ON_2$	100	16.85	17.1
	420–690°C	$C_4H_6N_2$	82	13.82	12.6
Remaining		Cu+CO_2	108	18.11	17.6

$(IMI)_2]$, the glu ligand was coordinated through the terminal part which consists of carboxylate and amine groups. Such coordination enabled the formation of aromatic-like ring and thus stabilizes the complex. This structural geometry is in agreement with the recently X-ray structure of $[Co(\mu\text{-glu})(nmim)_2]$ complex, where glu is glutarate and nmim is N-methylimidazole.[23] According to our calculations, all Co-Ligand bond lengths were slightly shorter than that of $[Co(\mu\text{-glu})(nmim)_2]$, as the Co-O(glu) bond length (1.92 Å) is shorter than Co-O(μ-glu) (1.96 Å). However, the differences in the bond angles were insignificant. The decrease in the bond lengths in our calculated complex is due to the formation of five-membered ring between Co and glu ligand. However, the similarity of the bond angles supported the idea that the disordered tetrahedral geometry is the most stable form of the complex.

Two octahedral models of Fe^{II} complex were calculated in which the imidazole molecules were modeled as *cis*- and *trans*-orientations. Table 4 summarizes the bond lengths and angles for all coordination bonds formed between the Fe^{II} and ligand molecules. Insignificant differences were observed for bond lengths in the two models. These distances were found to be slightly shorter than normal Fe-L bond distances[24] due to the formation of five-membered rings between Fe^{II} and glu ligand. Energetically, *trans*-$[Fe(glu)(IMI)_2(H_2O)_2]$ was found to be more stable than *cis*-$[Fe(glu)(IMI)_2(H_2O)_2]$ by about −14.07 kcal/mol. These results suggested that the Fe^{II} complex existed as *trans*-$[Fe(glu)(IMI)_2(H_2O)_2]$.

pH titrations

The potentiometric pH-titrations (25°C, 0.1 M $NaNO_3$) were carried out to obtain the acidity and stability constants which are summarized in Tables 5 and 6.

Metal-ligand stability constants of ternary complexes

The metal-ligand stability constants of the ternary complexes were evaluated assuming that the formation of hydrolyzed

Table 3. Infrared absorption bands frequencies (cm^{-1}) and electronic absorption spectra features of the prepared complexes.

Complex	υOH	μNH	$\mu CH_{aromatic}$	$\mu CH_{aliphatic}$	μCOO^{-}asy	μCOO^{-}sy	μM-N	μM-O	$\lambda_{max}\lambda$	$\varepsilon_{max}\varepsilon$	Assignment
GIMFe	3419	3150	3027	2934	1594	1437	619	435	410	1140	d-d band LMCT band
									370	860	Intraligand band
									360	840	Intraligand band
									345	780	
GIMCo	3442	3139	3049	2941	1604	1408	657	455	410	425	d-d band LMCT band
									405	487.5	Intraligand band
									395	637.5	
GDMCo	3436	3136	3035	2955	1598	1429	600	470	400	983.3	d-d band LMCT band
									350	833.3	
GIMCo	3401	3146	3041	2953	1623	1391	599	446	405	620	d-d band LMCT band
									350	550	
GLIMNi	3360	3130	3045	2860	1602	1405	625	502	420	775	d-d band LMCT band
									410	762.5	Intraligand band
									375	787.5	Intraligand band
									350	912.5	
GLDMCu	3431	3107	3052	2948	1595	1420	615	443	435	852	d-d band LMCT band
									405	746	Intraligand band
									375	921	Intraligand band
									350	872	
GDMCu	3417	3150	3044	2940	1593	1415	618	440	430	800	d-d band LMCT band
									345	975	
GMICu	3429	3115	3042	2934	1630	1415	614	474	400	900	d-d band LMCT band
									355	980	Intraligand band
									340	1240	

products, polynuclear complexes, hydrogen, and hydrogen bearing complexes were absent. An examination of titration curves (cf. Figures 2 and 3) indicates that complex formation has taken place in the solution on the following grounds:

1. The ternary complex titration curves show the displacement with primary complex titration curves. The horizontal distance was measured between acid curve and the secondary ligand curve (V_2–V_1) and subtracted through the horizontal distance between ternary complex curves and binary complex titration curves (V_4–V_3) show the positive difference, which proves the earlier releases of protons in the formation of ternary complexes. The hydrolysis of the metal ions was suppressed and precipitation did not result.
2. The color change of the ligand was in presence of metal ions appeared showing the formation of new species. From the ligand and metal titration curves the values of n and from that the values of PL were obtained. The formation curves obtained were used to evaluate the metal-ligand stability constants by Irving and Rossetti technique are presented in Tables 5 and 6. The variation of ṅ was found to be 0–2, which indicated that the composition of the complexes. The Irving-Williams order of stability constants was followed by both ligands.

DNA binding study using electronic absorption titration

DNA-binding studies can be conveniently monitored by absorption spectroscopy.[25] Hyperchromic and hypochromic effects are the spectra features of DNA concerning its double-helix structure.[26] This spectral change process reflects the corresponding changes of DNA in its conformation and structures after the drug bound to DNA. The spectra were recorded as a function of the addition of the buffer solutions of pre-treated CT-DNA to the buffer solutions of the complexes. If the binding mode is intercalation, the orbital of intercalated ligand can couple with the orbital of the base pairs, reducing the $\pi-\pi^*$ transition energy and resulting in bathochromism. If the coupling orbital is partially filled by electrons, it results in decreasing the transition probabilities and resulting in hypochromism.[16] The extent of the hypochromism in the metal-to-ligand charge transfer (MLCT) band is commonly consistent with the strength of intercalative interaction.[27–29] The electronic absorption spectra of GDMCu complex in the absence and presence of different concentration of buffered CT-DNA are given in Figure 4. By adding of DNA, the absorption intensities of MLCT band gradually increased. Moreover, addition of increasing amounts of CT-DNA resulted in a decrease of absorbance for each investigated complex. Representative spectra illustrating this hypochromicity and the presence of isosbestic points observed for the interaction of GDMCu complex with CT-DNA (cf. Figure 4). Table 7 shows binding constants for DNA interaction with the prepared complexes. It can be realized from the high percent of hypochromicity that the high strength binding of the prepared complexes with DNA. The investigated complexes could bind to DNA via an intercalative mode and showed a different activity with the sequence:

GLDMCu > GLIMNi > GCIMCo > GIMFe > GDMCo > GIMCo > GDMCu > GMICu.

The results revealed that the structure difference on the ligands and nature of metal ion might lead to obvious difference of DNA binding and intercalation abilities of the complexes.

DNA binding study with viscosity measurements

DNA viscosity is sensitive to DNA length change; therefore, its measurement upon addition of a compound is often concerned as the least ambiguous method to clarify the interaction mode of a compound with DNA and provides reliable evidence for the intercalative binding mode.[30,31] In the case of classic intercalation, DNA base pairs are separated in order to host the

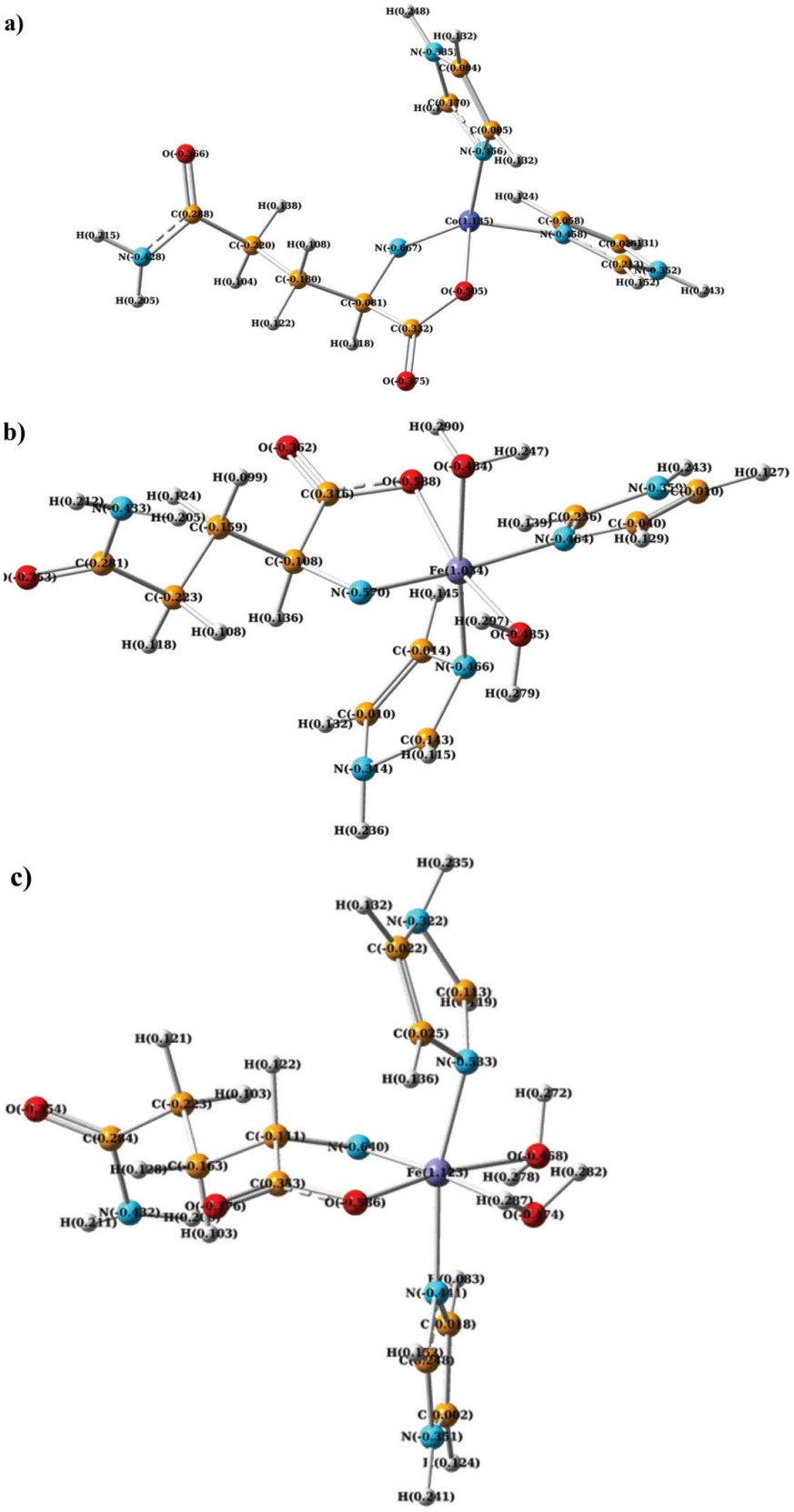

Figure 1. Optimized structures with the calculated atomic charges distribution of (a) $[Co(glu)(IMI)_2]$, (b) cis-$[Fe(glu)(IMI)_2]$, and (c) trans-$[Fe(glu)(IMI)_2]$ complexes.

bound compound resulting in the lengthening of the DNA helix and subsequently increased DNA viscosity. On the other hand, the binding of a compound exclusively in DNA grooves by means of partial or nonclassic intercalation causes a bend or kink in the DNA helix reducing its effective length and, as a result, DNA solution viscosity is decreased or remains unchanged.[32,33] The values of binding constant of the investigated complexes with DNA are smaller than that of reported

Table 4. Calculated bond distances (Å) and angles (°) of the coordination bonds for [M(glu)(IMI)$_2$] complex models.

L1—M—L2	L1—M	M—L2	L1—M—L2			
[Co(glu)(IMI)$_2$]						
O(glu)—Co—N(glu)	1.92	1.69	92			
O(glu)—Co—N(IMI1)	1.92	1.91	92			
N(glu)—Co—N(IMI1)	1.69	1.91	136			
O(glu)—Co—N(IMI2)	1.92	1.91	94			
N(glu)—Co—N(IMI2)	1.69	1.91	131			
N(imi1)—Co—N(IMI2)	1.91	1.91	92			
	Cis-			Trans-		
Cis-[Fe(glu)(IMI)$_2$.2H$_2$O]	L1—M	M—L2	L1—M—L2	L1—M	M—L2	L1—M—L2
O(glu)—Fe—N(glu)	1.87	186	94	1.88	1.81	96
O(glu)—Fe—N(IMI1)	1.87	1.92	86	1.88	1.91	86
N(glu)—Fe—N(IMI1)	1.86	1.92	173	1.81	1.91	91
O(glu)—Fe—N(IMI2)	1.87	1.86	110	1.88	1.87	97
N(glu)—Fe—N(IMI2)	1.86	1.86	100	1.81	1.87	102
N(IMI1)—Fe—N(IMI2)	1.92	1.86	86	1.91	1.87	165
O(glu)—Fe—O(W1)	1.87	2.03	161	1.88	2.04	171
N(glu)—Fe—O(W1)	1.86	2.03	86	1.81	2.04	91
O(glu)—Fe—O(W2)	1.87	2.04	73	1.88	2.08	87
N(glu)—Fe—O(W2)	1.86	2.04	83	1.81	2.08	173
N(IMI1)—Fe—O(W1)	1.92	2.03	91	1.91	2.04	88
N(IMI1)—Fe—O(W2)	1.92	2.04	90	1.91	2.08	83
N(IMI2)—Fe—O(W1)	1.86	2.03	89	1.87	2.04	87
N(IMI2)—Fe—O(W2)	1.86	2.04	175	1.87	2.08	84

for typical classical intercalators (EB-DNA; 3.3×10^5 L. mol^{-1}). The relative viscosity of DNA solution increases slightly as the amount of the complex increases, as shown in Figures 5a and 5b. This could be attributed to the insertion of aromatic ring of imidazol derivative ligands into the DNA base pairs and resulting in a bend in the DNA helix, hence an increase in separation of the base pairs at the intercalation site and increasing in DNA molecular length. Moreover, the sequence of the observed increase in the values of viscosity was correlated to the binding affinity to DNA (i.e., GLMDCu shows the highest binding affinity to DNA and the highest viscosity).[13,16,17]

Biological activity

The determination of antimicrobial susceptibility of a clinical isolate is often crucial for the optimal antimicrobial therapy of infected patients. This need is only increasing with increasing resistance and the emergence of multidrug-resistant microorganisms. Consequently, the synthesized complexes have been evaluated for their antimicrobial actions. The susceptibilities of certain strains of bacteria to Schiff base amino acid and their complexes were evaluated by measuring the size of the bacteriostatic diameter. The antimicrobial activity data of all synthesized compounds are summarized in Table 8 and show that the newly synthesized complexes possess biological activity. The results, thus obtained are explained on the basis of Overtone's concept and chelation theory.[27] The mode of action of the compounds may involve formation of a hydrogen bond through the azomethine group with the active centers of cell constituents, resulting in an interference with the normal cell process.[34] The antibacterial screening results exhibited marked enhancement in activity on coordination with the

Table 5. Metal-ligand stability constants of binary complexes.

	Cu(II)		Ni(II)	
Ligand (L)	log$K^M_{M(L)_2}$ N = 0.5	log$K^M_{M(L)}$ N = 1.5	log$K^M_{M(L)_2}$	log $K^M_{M(L)}$ N = 1.5
Glutamine	2.66	3.19	3.47	3.06
Glutamic	2.62	2.89	2.57	2.93
Glutaric	2.65	5.43	2.66	—

Table 6. Metal-ligand stability constants of ternary complexes.

Amino acids	metal	pH range	Log$K^M_{M(LA)}$
Glutamine	Cu(II)	8.4–11.7	3.16
Glutamic	Cu(II)	3.6–9.5	6.91
	Ni(II)	5.17–7.92	3.86
Glutaric	Ni(II)	4.83–6.34	3.16

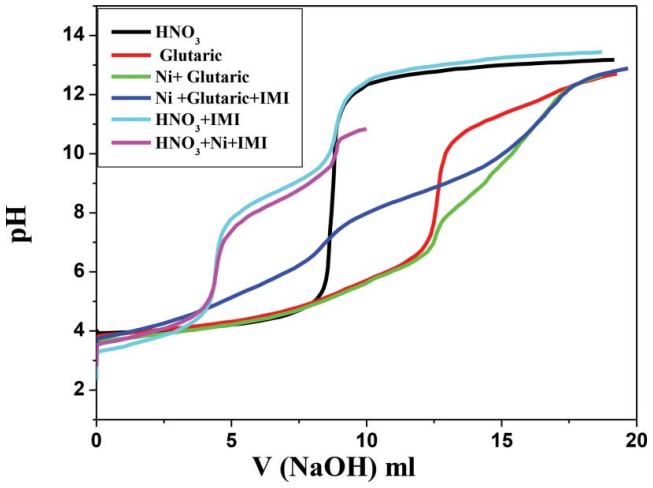

Figure 2. pH titration curves of glutaric acid, imidazole and Nickel ternary system in aqueous medium at 303 K and 0.1M ionic strength.

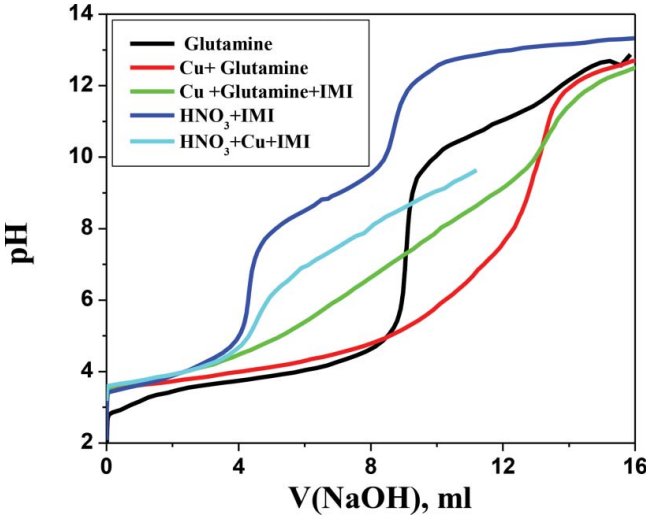

Figure 3. pH titration curves of glutamine, imidazole and copper ternary system in aqueous medium at 303 K and 0.1M ionic strength.

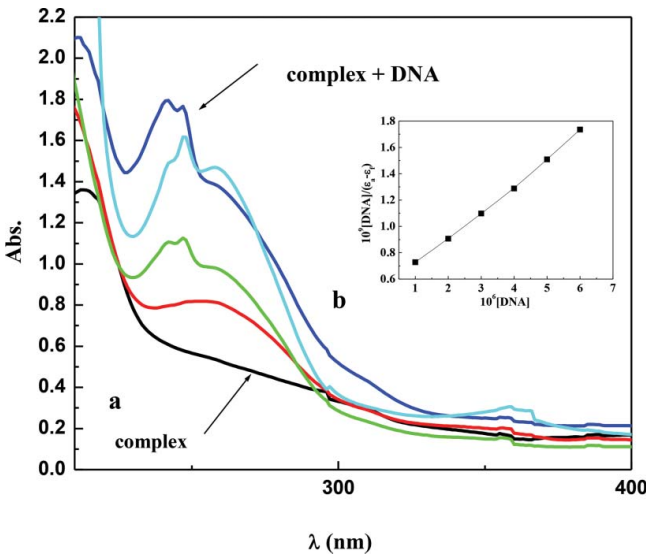

Figure 4. **(a)** Spectrophotometer titration of GDMCu complex (10^{-4} M) in 0.01 M Tris buffer (pH 7.4, 25°C) with CT-DNA from 0 μM (top) to 40 μM (bottom) CT-DNA with 5 μM intervals **(b)** Plot of [CT-DNA]/($\varepsilon_a - \varepsilon_f$) versus [CT-DNA] for the titration of CT-DNA with GDMCu complex.

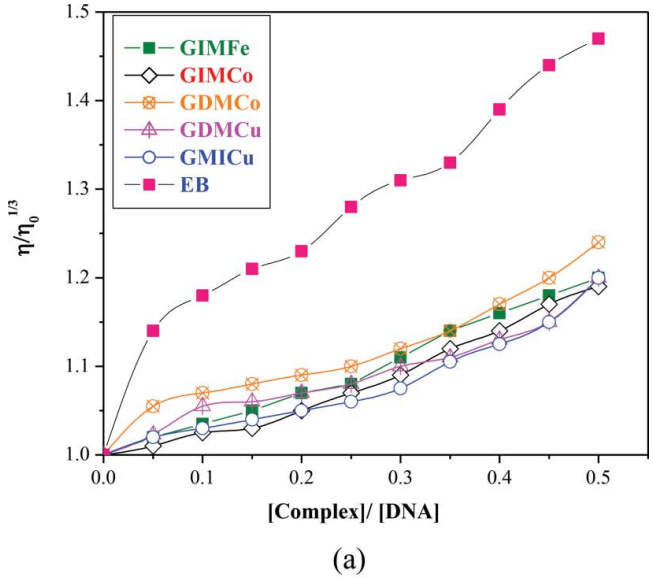

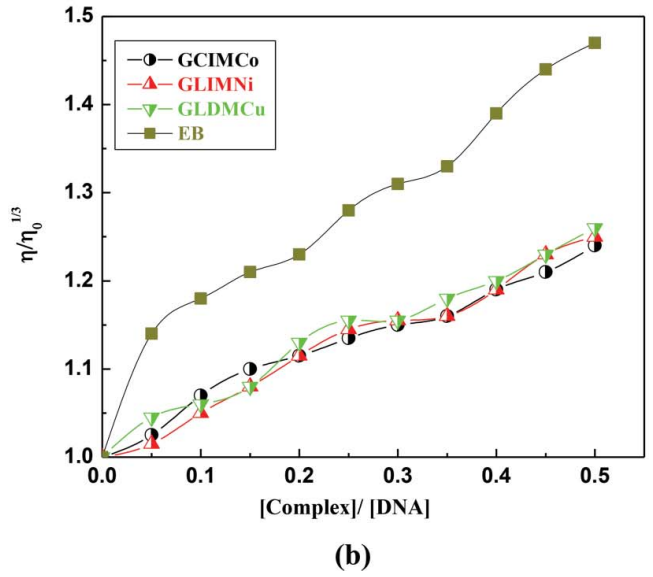

Figure 5. **(a, b)** The effect of increasing the amount of the synthesized complexes on the relative viscosities of DNA at [DNA] = 0.5 mM, [complex] and [EB] = 25–250 μM and 298 K.

metal ions against one or more testing bacterial strains (cf. Figures 6 and 7). This enhancement in the activity can be rationalized to the basis of the structures of the ligands by possessing an additional azomethine (C = N) linkage which is important in elucidating the mechanism of transamination and deamination reaction in biological system.[13,16,35] It has also been suggested[36] that the ligands with nitrogen and oxygen donor systems might inhibit enzyme production, as the enzymes that require these groups for their activity appear to be especially more susceptible to deactivation by the metal ions upon chelation. The polarity of the metal ion is reduced by chelation[37] and this is mainly because of the partial sharing of its positive charge with the donor groups and possibly with the delocalized π-electrons within the whole chelation ring, which is formed

Table 7. Binding constants and Gibbs free energy for DNA interaction with the synthesized complexes.

	GIMFe	GIMCo	GDMCo	GDMCu	GMICu	GCIMCo	GLIMNi	GLDMCu
Binding constant $K_b \times 10^3$ M^{-1}	6.39	6.01	6.25	5.83	5.65	6.80	7.11	7.75
$\Delta G^{\neq}$ kJ mol^{-1}	−21.71	−21.56	−21.65	−21.48	−21.36	−21.86	−21.97	−22.19

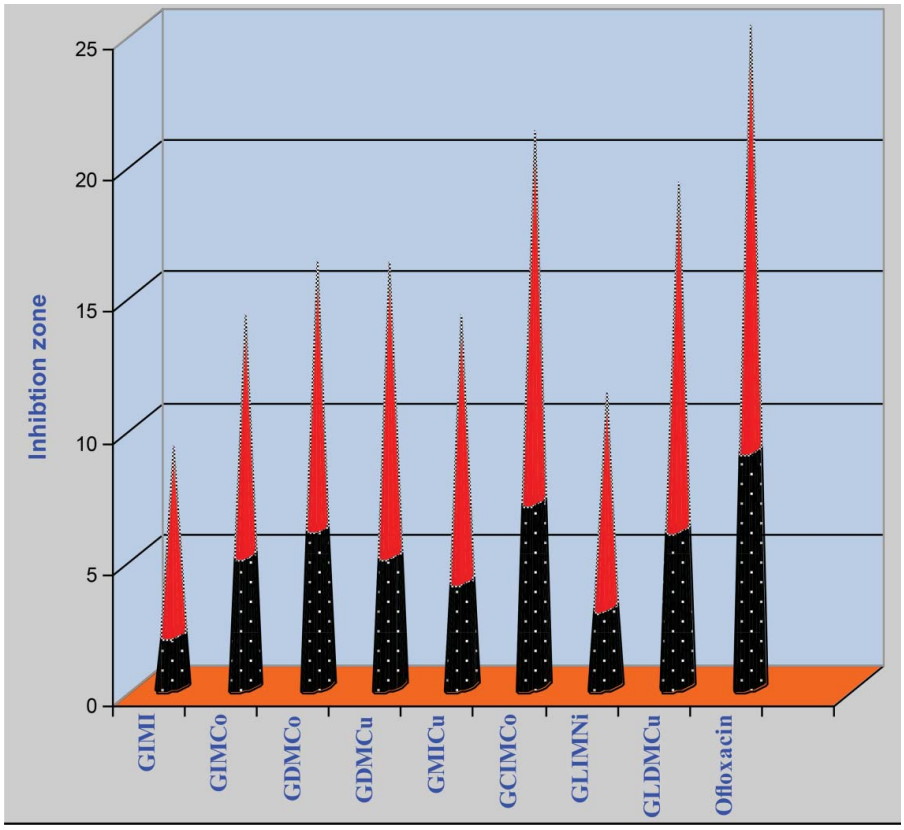

Figure 6. Antibacterial evaluation of the investigated complexes against *Pseudomonas aeruginosa* bacteria.

because of the coordination. This process of chelation increases the lipophilic nature of the central metal atom, which in turn favors its permeation through the lipoid layer of the membrane.[38] This is also responsible for the increasing of the hydrophobic character and liposolubility of the molecules in crossing the cell membrane of the microorganism and hence enhances the biological utilization ratio and activity of the testing drug/compound. Moreover, it was found that the prepared compounds show moderate to high activity compared to the standard drugs used in the investigation (cf. Tables 8 and 9)

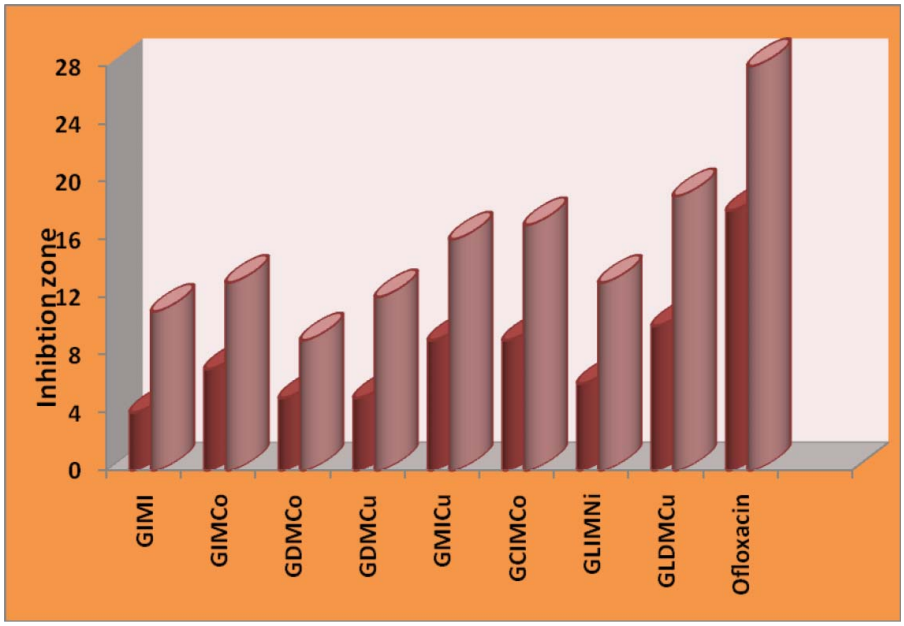

Figure 7. Antibacterial evaluation of the investigated complexes against *B. cereus* bacteria.

Table 8. Results of antimicrobial activity[a] of the ligands and their metal complexes in DMSO.

Compound	*P. aeruginosa*			*B. cereus*		
Conc. (mg/ml)	5	10	20	5	10	20
GIMFe	2	4	7	4	6	11
GIMCo	5	7	9	7	9	13
GDMCo	6	8	10	5	8	12
GDMCu	5	6	11	9	13	16
GMICu	4	7	10	7	10	14
GCIMCo	7	10	14	9	12	17
GLIMNi	3	5	8	6	6	13
GLDMCu	6	9	13	10	15	19
Ofloxacin	8	13	16	18	23	28
Ciprofloxacin	9	12	17	19	24	35

[a]Values of inhibition zone (in mm) are ± 0.23 and average of three replicates.

Table 9. Results of activity index (%) for antibacterial assay of the prepared complexes.

	Activity index (%)	
Compounds	*P. aeruginosa*	*B. cereus*
GIMFe	43.75	39.28
GIMCo	52.94	46.29
GDMCo	58.82	42.86
GDMCu	64.71	57.14
GMICu	58.82	50.00
GCIMCo	82.35	60.71
GLIMNi	40.06	46.42
GLDMCu	76.47	67.86

Conclusion

Ternary metal(II) complexes incorporating amino acid and imidazol derivatives were prepared and characterized by different techniques. The structure of $[Co(glu)(IMI)_2]$ and $[Fe(glu)(IMI)_2(H_2O)_2]$ complexes was validated using quantum mechanics calculations based on accurate DFT methods. Moreover, The DNA electrophoretic mobility studies show that the compounds interact with DNA either most probably by an intercalative mode or by a simple mode of coordination (leading to creation of high molecular weight (DNA complexes) contributing to the formation of DNA catenanes and subsequently promoting double stranded-scissions to DNA acting also as chemical nucleases. These findings clearly indicate that transition metal–based complexes have many potential practical applications, such as the development of nucleic acid molecular probes and new therapeutic reagents for diseases. Furthermore, the prepared metal(II) complexes show a good antibacterial activity.

Funding

The authors are deeply grateful to the University of Oviedo and Sohag University for supporting and facilitating this study.

References

1. Nelson, D. L.; Cox, M. M. *Lehninger Principles of Biochemistry*, 3rd edn.; Worth, New York, 2000.
2. Chen, P. E.; Geballe, M. T.; Stansfeld, P. J.; Johnston, A. R.; Yuan, H.; Jacob, A. L.; Snyder, J. P.; Traynelis, S. F.; Wyllie, D. J. A. *Mol. Pharmacol.* **2005**, *67*, 1470–1484.
3. Sajadi, S. A. A. *Adv. Biosci. Biotechnol.* **2010**, *1*, 354–360.
4. Xiao, S.; Textor, M.; Spencer, N. D.; Sigrist, H. *Langmuir* **1998**, *14*, 5507.
5. Konishi, Y.; Shimaoka, J.; Asai, S. *React. Funct. Polym.* **1998**, *36*, 197.
6. Fisher, G.; Lorenzo, N.; Abe, H.; Fujita, E.; Frey, W. H.; Emory, C.; Di Fiore; M. M.; D'Aniello, A. *Amino Acids* **1998**, *15*, 263.
7. D'Aniello, A.; Fisher, G.; Migliaccio, N.; Cammisa, G.; D'Aniello, E.; Spinelli, P. *Neurosci. Lett.* **2005**, *49*, 388.
8. Lah, N.; Cigic, I. K.; Leban, I. *Inorg. Chem. Commun.* **2003**, *6*, 1441.
9. Yu, Z. W.; He, M. H.; Zhang, W.; Sun, P. *Chin. J. Struct. Chem.* **2010**, *29*, 1301.
10. Li; H. Q.; Xian, H. D.; Zhao, G. L. *J. Rare Earths* **2010**, *28*, 7.
11. Chabner, B. A.; Roberts, T. G. *Nat. Rev. Cancer* **2005**, *5*, 65.
12. Indumathy, R.; Radhika, S.; Kanthimathi, M.; Weyhermuller, T.; Nair, B. U. *J. Inorg. Biochem.* **2007**, *101*, 434.
13. Abdel-Rahman, L. H.; El-Khatib, R. M.; Nassr, L. A. E.; Abu-Dief, A. M. *J. Mol. Struct.* **2013**, *1040*, 9–18.
14. Frisch, M. J. et al.; *Gaussian 03, Revision C.01*; Gaussian, Inc., Wallingford, CT, 2004.
15. Ditchfield, R.; Hehre, W. J.; Pople, J. A. *J. Chem. Phys.* **1971**, *54*, 724–728.
16. Abdel-Rahman, L. H.; El-Khatib, R. M.; Nassr, L. A. E.; Abu-Dief, A. M.; Ismael, M.; Seleem, A. A. *Spectrochim. Acta* **2014**, *117*, 366–378.
17. Abdel-Rahman, L. H.; El-Khatib, R. M.; Nassr, L. A. E.; Abu-Dief, A. M.; Lashin, F. E. *Spectrochim. Acta* **2013**, *111*, 266–276.
18. Satyanarayana, S.; Dabroniak, J. C.; Chaires, J. B. *Biochemistry* **1992**, *31*, 9319.
19. Raman, N.; Kulandaisamy, A.; Jeyasubramanian, K. *Synth. React. Inorg. Met.-Org. Chem.* **2001**, *31*, 1249–1260.
20. Hu, R.; Yu, Q.; Liang, F.; Ma, L.; Chen, X.; Liang, H.; Yu, K. *J. Coord. Chem.* **2008**, *61*, 1265.
21. Choi, K. Y.; Jeon, Y. M.; Ryu, H.; Oh, J. J.; Lim, H. H.; Kim, M. W. *Polyhedron* **2004**, *23*, 903–911.
22. Lever, A. B. P. *Inorganic Electronic Spectroscopy*; Elsevier, Amsterdam, 1968.
23. Yesilel, O. Z.; Kılıc, Y.; Sahin, O.; Buyukgungor, O. *Polyhedron* **2014**, *67*, 122–128.
24. Jameson, G. B.; Molinaro, F. S.; Collman, J. P.; Brauman, J. I.; Rose, E.; Suslick, K. S. *J. Am. Chem. Soc.* **1978**, *100*, 6769–6770.
25. Johnson, J. E. B.; Ruminski, R. R. *Inorg. Chim. Acta* **1993**, *208*, 231.
26. Li, Q. S.; Yang, P.; Wang, H. F.; Guo, M. L. *J. Inorg. Biochem.* **1996**, *64*, 181–195.
27. Liu, X. W.; Li, J.; Li, H.; Zheng, K. C.; Chao, H.; Ji, L. N. *J. Inorg. Biochem.* **2005**, *99*, 2372–2380.
28. Abdel Rahman, L. H.; Abu-Dief, A. M.; Hamdan, S. K.; Seleem, A. A. *Int. J. Nano. Chem.* **2015**, *1*, 65–77.
29. Abu-Dief, A. M.; Nassr, L. A. E. Tailoring, physicochemical characterization, antibacterial and DNA binding mode studies of Cu(II) Schiff bases amino acid bioactive agents incorporating 5-bromo-2-hydroxybenzaldehyde. *J. Iranian Chem. Soc.* **2015**, *12*, 943–955.
30. Li, D.; Tian, J.; Gu, W.; Liu, X.; Yan, S. *J. Inorg. Biochem.* **2010**, *104*, 171–179.
31. Garcia-Gimenez, J. L.; Gonzalez-Alvarez, M.; Liu-Gonzalez, M.; Macias, B.; Borras, J.; Alzuet, G. *J. Inorg. Biochem.* **2009**, *103*, 923–934.
32. Kelly, J. M.; Tossi, A. B.; McConnell, D. J.; Uigin, C. O. *Nucl. Acids Res.* **1985**, *13*, 6017–6034.
33. Pyle, A. M.; Rehmann, J. P.; Meshoyrer, R.; Kumar, C. V.; Turro, N. J.; Barton, J. K. *J. Am. Chem. Soc.* **1989**, *111*, 3051–3058.
34. Liu, J.; Zhang, H.; Chen, C.; Deng, H.; Lu, T.; Li, L. *Dalton Trans.* **2003**, 114–119.
35. Abdel-Rahman, L. H.; Abu-Dief, A. M.; Hashem, N. A.; Seleem, A. A. Recent advances in synthesis, characterization and biological activity of nano sized Schiff base amino acid M(II) complexes. *Int. J. Nano. Chem.* **2015**, *1*, 79–95.
36. Nishat, N.; Hasnain, S.; Asma, S. D. *J. Coord. Chem.* **2010**, *63*, 3859–3870.
37. Rehman, S. U.; Chohan, Z. H.; Naz, F.; Supuran, C. T. *J. Enzyme Inhib. Med. Chem.* **2005**, *20*, 333–340.
38. Chohan, Z. H.; Arif, M.; Shafiq, Z.; Yaqub, M.; Supuran, C. T. *J. Enzyme Inhib. Med. Chem.* **2006**, *21*, 95–103.